Journal of Hazardous Materials 167 (2009) 250–259

Contents lists available at ScienceDirect

Journal of Hazardous Materials

journal homepage: www.elsevier.com/locate/jhazmat

Hydrothermal processing of MSWI Fly Ash-towards new stable minerals and fixation of heavy metals

A.P. Bayuseno[a,*,1], W.W. Schmahl[b], Th. Müllejans[c]

[a] Institute for Mineralogy, Geology and Geophysics, Ruhr-University of Bochum, Germany
[b] Department of Geo- and Environmental Sciences, Ludwig-Maximilians University of München, Germany
[c] MVA Iserlohn, Germany

ARTICLE INFO

Article history:
Received 14 July 2008
Received in revised form
23 December 2008
Accepted 24 December 2008
Available online 31 December 2008

Keywords:
Hydrothermal processing
MSWI fly ash
Tobermorite
Chemical stability

ABSTRACT

A hydrothermal processing strategy of MSWI fly ash is presented for obtaining stable minerals with low toxic potential. Different hydrothermal conditions were tested to obtain high yields of new stable minerals. Experimental parameters including temperature, nature and molarity of alkali reagents, and reaction time were evaluated. The chemical stability of hydrothermal products was examined by the toxicity characteristic leaching procedure (TCLP) test and subsequent XRD for the leached residue. The significant amounts of Al-substituted 11 Å tobermorite and katoite in addition to minor amounts of zeolites were formed under experimental conditions at 0.5 M NaOH, 180 °C for 48 h, however KOH treatment in a similar regime resulted in smaller amounts of Al-substituted 11 Å tobermorite and katoite. Similarly, a product of mixed Al-substituted 11 Å tobermorite and katoite could be formed from the washed fly ash treated in 0.5 M NaOH at 180 °C for 48 h. Under the acidic condition, the treated fly ash exhibited an excellent stability of the mineral assemblage and less release of heavy metals relative to the untreated parent materials.

1. Introduction

MSWI residues represent a by-product generated from municipal solid waste incineration and they are comprised primarily of: (i) bottom ash and (ii) fly ash [1,2]. Bottom ash is not classified as a hazardous waste according to the European Waste Catalogue, and it is explored frequently for constructional applications. It has been recycled commonly in Germany as a secondary building material for civil engineering applications. Utilization of fly ash, however, is at present realized in low technology applications such as additive in cement and construction materials. In Germany, disposal of fly ash is realized by wetting with water which leads to a puzzolanic solidification of the ash in the waste disposal site. Disposal or low level of ash utilization is inevitable due to the potential leachability of heavy metals (Cd, Zn, Pb, Hg, Cu, Cr and Ni) and toxic organic compounds to the environment [3–6]. In addition, fly ash is very highly reactive and subject to mineralogical alteration when it is in contact to the environment. The potential instability in the environment makes it difficult for fly ash to compete with alternative raw materials. Hence for providing a possible utilization of fly ash, chemical stabilization of this material is required. This makes eventually a positive impact on the waste minimization and the reduction of waste accumulation at landfills [5].

Various technological options such as thermal treatment, physical/chemical separation, and stabilization/solidification (S/S) techniques are now available for treatments of fly ash in view of their reuse or final disposal [7–10]. The use of thermal treatment via vitrification has been tested and practised on a small scale. However, the method is considered more costly than other solutions because it requires a significant amount of energy and an expensive capital apparatus. It could also lead to a subsequent environmental destructive impact as a result of volatilisation of heavy metals from fly ash during vitrifying and melting processes.

As an alternative to the thermal treatment, physical/chemical separation methods employed for extracting heavy metals (Cd, Pb and Zn) from fly ash have been attempted but with limited success [11–13]. More recently, the stabilization and solidification (S/S) methods have emerged as a viable alternative for MSWI fly ash treatment by solidification with Portland cement into stable complexes [14]. In this context, toxic components are incorporated in a cement matrix through either physical or chemical immobilization mechanisms, depending on the particular contaminant to be fixed and type of binder being used. This technique has long been known as an economical option for the waste management strategy [14].

* Corresponding author. Present address: Department of Mechanical Engineering, Diponegoro University, Kampus Tembalang, Semarang 50255, Indonesia.
Tel.: +62 24 7460059; fax: +62 24 7460059.
E-mail address: abayuseno@yahoo.com (A.P. Bayuseno).
[1] Supported by the KAAD (Katholischer Akademischer Austausch Dienst) Bonn, Germany.

0304-3894/$ – see front matter © 2008 Elsevier B.V. All rights reserved.
doi:10.1016/j.jhazmat.2008.12.119

However, the solidification with Portland cement presents some disadvantages. Specifically protection against humidity is required to prevent breakdown and leaching of heavy metals [15]. In addition, salts present in fly ash will interfere with basic hydration reactions of cement, leading to an inadequate set and/or deterioration of the waste form over time.

Pozzolanic solidification of MSWI fly ash in a solution enriched with $Ca(OH)_2$ in order to take an advantage of its pozzolanic property has yet to be fully realized [16,17]. An interesting potential for generating a pozzolanic property of MSWI fly ash is that ettringite and calcium-silicate-hydrate (C-S-H) may be formed using an activator of $Ca(OH)_2$ giving a good degree of stabilization of the hardened material. This stabilized material becomes, in principle, more compatible for storage, landfill or reuse as a resource.

Among other ash treatments, a hydrothermal method for processing fly ash with improved chemical stability could be considered as a promising technology, which offers considerable advantages in terms of economic, technical and environmental performance [5]. This method has been employed successfully for treating coal fly ash in alkali solutions (NaOH and KOH), [18], and may be also beneficially applied for MSWI fly ash. The value in using MSWI fly ash in the synthesis of zeolites is due to its high specific surface and high content of aluminosilicate glass [5], although this glass may be less abundant in MSWI fly ash than in coal fly ash. Further, the efficiency of hydrothermal processing depends upon the mass ratio of SiO_2 and Al_2O_3-components in the glassy phase which has the greatest influence over the composition and type of stable minerals produced [19].

Recent publications on the hydrothermal treatment of MSWI fly ash have improved understanding considerably for new potential applications of fly ash as resources [20–22]. The use of MSWI fly ash for the synthesis of zeolite compounds (*e.g.*, zeolites A and P and Sodalite) by the hydrothermal method in the NaOH solution has been demonstrated previously [20,22]. Here water washing was previously employed for the treatment of fly ash and followed by heating of fly ash at 800 °C. This pre-treatment procedure is suggested to be an important part for the preparation of reproducible zeolitic compounds. Yao et al. [23] have reported the synthesis of tobermorite [$Ca_5Si_6(OH)_2O_{16}{\cdot}4H_2O$] from fly ash by hydrothermal treatment in NaOH solutions at 180 °C, and those products revealed the uptake behavior for Cs^+ and NH_4^+. More recently, a mixture of Al-substituted tobermorite-11 Å [$Ca_5(Si,Al)_6(OH)_2O_{16}{\cdot}4H_2O$] and katoite [$Ca_3Al_2(SiO_4)(OH)_8$] has been synthesized from newsprint recycling residues under hydrothermal condition at 100 °C in NaOH, LiOH and KOH solutions [24]. The resulting products of Al-substituted tobermorite-11 Å and katoite facilitated the immobilization of heavy metal ions and also exhibited an important ion exchange property for nuclear and hazardous wastewater conditioning. However, characteristics of MSWI fly ash, which are essential to provide a scientific basis and establish confidence in the technology of hydrothermal processes, remain poorly understood and lack quantification. This is probably because of complicated chemical and mineralogical character of fly ash. A detailed knowledge of mineralogical phase compositions (crystalline and glassy phases) of fly ash is necessary in order to be able to assess the correlation between microstructure and process parameter and thus, to optimize the stabilized products.

The present study was undertaken to access the benefits of hydrothermal processing of MSWI fly ash to stable phase minerals. The starting fly ash was hydrothermally treated in 0.5 M NaOH and KOH solution at temperatures ranging 90–180 °C for 48 h. Parallel experiments were also conducted with the washed fly ash. These experimental conditions were chosen on the basis of our study [25] indicating that the best crystallinity of stable mineral phases (*i.e.*, tobermorite-11 Å, and katoite) would be formed at such experimental conditions. Effects of temperatures on the processing of amorphous and crystalline phases to stable mineral phases were analyzed by the Rietveld refinement method from X-ray diffraction (XRD) data. The resulting products were also characterized by scanning electron microscopy (SEM) for microstructure and morphology observation, and by the toxicity characteristic leaching procedure (TCLP) for testing of hazardous materials.

2. Experimental procedure

2.1. Materials

Approximately 5 kg of MSWI fly ash were collected from the electrostatic precipitator (ESP) facility at an incinerator plant of the town of Iserlohn close to the Ruhr industrial area, Germany. This sampled fly ash was then homogenized within 24 h after sampling with an agate vibratory disc mill for 30 min, until all material had passed a 100 μm sieve. LOI was determined by heating the raw fly ash to constant weight at 750 °C.

A pre-treatment of fly ash was conducted by water-washing in a glass beaker equipped with a magnetic stirrer for mixing at 300 rpm. Batches of 70 g of the fly ash powder were prepared in this way. They were initially placed in the glass beaker containing distilled water. The water to solid mass ratio (ml/g) was adjusted to be 10. Subsequently, this mixture was stirred to stand for 24 h

Table 1
Chemical composition of raw and washed fly ashes.

Element	Raw fly ash	Washed fly ash
	Wt.%	
Si	5.63 (20)[a]	6.95 (25)
Ti	1.02 (02)	1.53 (05)
Al	2.43 (02)	3.73 (06)
Fe	3.71 (05)	3.99 (08)
Ca	12.41 (22)	18.97 (26)
Mg	1.08 (02)	1.57 (04)
Mn	0.12 (0)	0.18 (02)
K	6.11 (08)	0.99 (01)
Na	10.38 (28)	3.09 (07)
P	0.40 (0)	0.55 (0)
Cl	8.32 (14)	0.56 (0)
Pb	1.36 (07)	2.17 (09)
S	4.12 (0)	5.49 (0)
Zn	4.91(03)	8.09(08)
[b]LOI	8.51(28)	
Element	Raw fly ash	Washed fly ash
	ppm	
As	307 (25)	1029(30)
Ba	3470 (93)	5365(75)
Bi	204 (2)	364(5)
Cd	456 (6)	751 (7)
Co	262 (18)	265 (19)
Cr	2026 (29)	2924 (39)
Cs	114 (3)	184 (5)
Cu	3513 (32)	5660 (24)
F	1 (0)	5131 (28)
Ga	3042 (229)	43 (0)
Mo	30 (4)	609 (4)
Ni	9 (1)	799 (21)
Rb	34 (1)	27 (2)
Sb	3 (0)	2678 (2)
Sn	489 (7)	557 (8)
Sr	24 (4)	744 (6)
V	614 (19)	122 (14)
Y	6 (3)	1436 (24)
Zr	265 (3)	336 (7)

[a] Figures in parentheses indicate the least-squares estimated standard deviation (esd) referring to the least significant figure to left, a zero indicates an esd < 0.05%.
[b] LOI: loss on ignition.

at room temperature. At the end of stirring, the resulting slurries was filtered with a paper filter (Schleicher & Schuell no. 604), washed repeatedly with distilled water, and dried at room temperature for subsequent hydrothermal experiments. The wastewater was collected for subsequent volume reduction by water evaporation to a solid residue for disposal. The main reason for washing was to remove as much chloride possible. It was expected that the chloride-salts present in the fly ash would reduce the efficiency of the hydrothermal treatment. This suggestion, however, had not significantly changed the results focused on the efficiency of the hydrothermal treatment in this work.

The bulk chemical compositions of the raw and washed fly ash powders were then determined by wavelength dispersive X-ray fluorescence (XRF) and are provided in Table 1. The phase abundance of the raw and washed fly ashes, estimated from powder XRD traces using the Rietveld refinement method [26], is given in Table 2. The term "amorphous" in this table refers largely to the XRD glassy material but may include small quantities of unidentified crystalline minerals.

2.2. Hydrothermal experiment

The raw and washed fly ashes were used as Si^{+4} and Al^{+3}-sources for the hydrothermal synthesis of stable mineral phases. For the experiment, batches of 15 g of the fly ash powder were prepared and then mixed with an alkali solution (either KOH or NaOH) in a glass beaker, of which the liquid/solid (L/S) ratio was adjusted to be 10 ml/g. The mixture was further stirred with a magnetic stirrer at 300 rpm for 24 h.

The hydrothermal experiment was conducted without stirring in a Teflon-line autoclave under an autogenous pressure. The reaction temperatures (90–180 °C), reaction time (48 h), and 0.5 M of alkali metal hydroxide solutions were selected as control parameters. After the experimental treatments, the reaction mixtures were filtrated through a paper filter (Schleicher & Schuell no. 604) and centrifuged. The resulting slurries were dried at room temperature. The dried cake products were then ground and stored in airtight polypropylene containers until analyzed.

2.3. Characterization

The hydrothermal products were characterized by various conventional methods. Scanning electron microscopy (SEM) supported by EDX was used for characterizing the microstructure and morphology. For the investigation, the specimens were mounted onto aluminium stubs using double-sided adhesive carbon discs and sputter coated with gold.

X-ray diffraction (XRD) analysis was performed using Cu Kα monochromated radiation in a conventional Bragg-Brentano (BB) parafocusing geometry (Siemens D500 and Philips X-Pert Diffractometer). The accelerating voltage was 45 kV, and the current was 30 mA. The scan parameters (5–85° 2θ in 0.020° increments, 10–15 s/step) were selected as required for observation. Data were recorded digitally, and peak positions and intensities were identified by using the peak search finder feature or on screen in the software. Initially, a PC-based search match program, the Philips X'Pert Software (Philips Electronics N.V.) involving the ICDD-PDF database as a source of reference data was employed to help identify possible crystalline phases in the ash samples. The crystalline phase identified by search match procedures were subsequently employed for the Rietveld full profile fitting analysis, [26] in addition to the quantitative XRD phase analysis. The Rietveld method was selected for our study because: (i) quantitative information for minor phases was desired, (ii) significant (sometimes total) overlapping peaks were present in samples, and (iii) best confidence in the reliability of result was desired.

The Rietveld calculations were performed using the SIROQUANT *Quantitative XRD software* program [27]. The SIROQUANT contains an extensive database of crystal structure models from which the full diffraction profiles are calculated. Additional structure models were also taken from the Inorganic Crystal Structure Database (ICSD). The strategy adopted made use of refinements of the diffraction data collected from samples (i) without internal standard and (ii) with internal standard for amorphous phase determination. The wt.% levels of mineralogical phases including the glass content were derived using an internal standard Rietveld procedure [28] with CeO_2 (NIST SRM 674) as the internal standard material. The amorphous level or glassy phase content was then determined by the difference between the sum of the weight fractions for all phases and 100%. Detailed discussion of the calculation method is presented elsewhere [25].

2.4. Leaching test

A single step leaching test was performed according to the standard of the toxicity characteristic leaching procedure (TCLP) of the Environmental Protection Agency (U.S. EPA, 1990) (EPA-SW 846 Method 1311) [29]. 10 g of the powder batches were initially ground to particles less than 200 μm in size. The ground sample was subsequently extracted by using an acetic acid solution (CH_3COOH supplied by J.T. Baker, Holland) mixed with distilled water. The solution with a liquid-to-solid mass (L/S) ratio of 20:1 (ml/g) was selected and the time of extraction was 18 ± 3 h. Here, the acetate buffer was added only once in order to have a solution with pH of 3, at the start of the extraction. The mixture was then stirred in a glass beaker using a magnetic stirrer at 300 rpm. After the leaching process, the leachants were filtered through a paper filter (Schleicher & Schuell no. 604) and pH was again measured prior to conducting chemical analysis. The concentrations of heavy metals in the leachants were determined by inductively coupled plasma mass spectroscopy (ICP-MS), while the dried filter cakes of the leached ash were then examined by XRD.

3. Results

3.1. Hydrothermal processing of raw fly ash

The raw fly ash contained an amorphous phase as the major phase plus various SiO_2 and Al_2O_3-bearing phases such as quartz and gehlenite (Table 2). More than 55 wt.% of the sample consisted aluminosilicate glass, which is probably Ca-rich. Other minerals such as magnetite, hematite, chloride minerals and Ca-sulfates are considered as impurities for the study as they do not contribute to the formation of zeolites or neomorphic phases.

X-ray diffractograms of the raw fly ash hydrothermally treated at temperatures 90–180 °C in 0.5 M NaOH for 48 h are given in Fig. 1a. The XRD signals of Fig. 1a provide direct experimental evidence of the minerals composing the fly ash and of the new minerals formed in the treatment products. Halite, anhydrite and sylvite previously detected in the raw sample are absent at 90 °C. Correspondingly, the new secondary minerals hydrocalumite [$Ca_8Al_4(OH)_{24}(CO_3)(Cl)(H_2O)_{9.6}$] and monosulfate ($3CaO{\cdot}Al_2O_3{\cdot}CaSO_4{\cdot}12H_2O$) were formed (strongest peaks at 11.19° 2θ, PDF#78-2051 and 9.89° 2θ, PDF#83-1289, respectively). Hence, synthesis at 90 °C yielded a relatively high proportion of hydrocalumite and a small proportion of monosulfate, together with a dramatic reduction of anhydrite, bassanite, halite and sylvite. It seems that the formation of monosulfate is likely related to the decomposition of ettringite, as this phase is unstable above a temperature of 90 °C [30]. In addition, portlandite and iron hydroxide (lepidocrocite, FeOOH) were identified. Ca-bearing minerals

Table 2
XRD-based mineralogy of the raw and washed fly ashes.

Mineral phase (wt.%)	Formula	Raw fly ash	Washed Fly ash	Structure model[a]
Amorphous		57.4(9)[b]	47.2(6)	
Albite (plagioclase)	$NaAlSi_3O_8$	1.1(2)	6.3(3)	S-155
Alunite	$NaKAl_3(OH)_6(SO_4)_2$	1.4(1)		S-459
Anhydrite	$CaSO_4$	4.5(3)	5.2(1)	S-80
Apatite	$Ca_5(PO_4)_3OH$	2.0(2)		S-215
Augite	$Ca_3Na_3Mg_3FeAl_{1.6}Si_7O_{24}$		1.7(2)	S-622
Bassanite	$CaSO_4{\cdot}0.5H_2O$	0.7(1)		S-292
Calcite	$CaCO_3$	1.7(2)	3.3(1)	S-11
Caracolite	$Na_3Pb_2(SO4)_3Cl$	0.4(1)		I-024459
Calcium titanite	$CaTiO_3$	0.4(1)		S-757
C_3A	$Ca_3Al_2O_6$	0.9(1)	0.6(1)	S-71
C_2S	Ca_2SiO_4	0.8(1)	0.7(2)	S-69
C_3S	Ca_3SiO_5	0.9(2)	0.8(2)	S-128
Diopside	$CaMgSi_2O_6$	1.8(2)		S-133
Enstatite	$(Mg,Fe)SiO_3$	1.2(2)		S-151
Ettringite	$3CaO{\cdot}Al_2O_3{\cdot}3CaSO_4{\cdot}32H_2O$		1.4(1)	S-195
Forsterite (olivine)	$(Mg,Fe)_2SiO_4$	2.0(2)		S-53
Garnet	$Ca_3(Al,Fe)_2(Si,P)_3O_{12}$	0.4(1)		S-552
Gehlenite (melilite)	$(Ca,Na)_2(Mg,Fe,Si,Al)_3O_7$	1.4(2)	2.9(1)	S-165
Gordaite	$NaZn_4(SO_4)(OH)_6Cl(H_2O)_6$		0.5(1)	I-406090
Gypsum	$CaSO_4{\cdot}2H_2O$		16.4(2)	S-355
Halite	NaCl	5.3(1)		S-105
Hematite	Fe_2O_3	1.8(1)	0.8(1)	S-41
Hydrocalumite	$Ca_8Al_4(OH)_{24}(CO_3)(Cl)\,(H_2O)_{9.6}$	0.7(1)	2.1(1)	S-778
Illite	$KAl_3Si_3O_{10}(OH)_2$	0.4(0)		S-116
Iron	Fe	0.5(1)		S-140
Kalsilite	$KAlSiO_4$	0.3(0)	1.9(0)	S-961
Lepidocrocite	FeOOH		0.6(1)	S-45
Marcasite	FeS_2		0.4(1)	S-362
Minium	Pb_3O_4	0.8(1)	0.3(0)	S-713
Magnetite	Fe_3O_4	0.9(1)	1.5(1)	S-50
Nepheline	$Na_3KAl_4Si_4O_{16}$	1.2(2)	1.0(1)	S-89
Portlandite	$Ca(OH)_2$	0.4(1)		S-124
Pyrite	FeS_2	0.5(1)		S-29
Quartz	α-SiO_2	1.5(1)	2.0(1)	S-1
Rutile	TiO_2	0.9(1)	0.7(1)	S-15
Sanidine	$KAlSi_3O_8$	2.0(3)		S-21
Sodalite	$Na_4Al_3Si_3O_{12}Cl$	0.4(1)	0.5(1)	S-1031
Sylvite	KCl	1.2(1)		S-164
Tobermorite-14 Å	$Ca_5(OH)_2SiO_{16}{\cdot}4H_2O$	0.5 (1)		S-309
Ulvöspinel	Fe_2TiO_4	0.9(1)	1.2(1)	S-362
Zinc Chloride	$ZnCl_2$	0.8(0)		S-5
Total		100	100	

[a] The reference is given as a letter S for the SIROQUANT database (2002) and I for the ICDD followed by the entry number of the respective database.
[b] Figures in parentheses indicate the least-squares estimated standard deviation (esd) referring to the least significant figure to left, a zero indicates an esd < 0.05%.

(*e.g.*, gypsum and anhydrite), magnetite and hematite remained constant with rising temperature and they were still present in the hydrothermal product. Moreover, gehlenite, which is expected to play an important role in providing the Ca^{2+}-ion, remained unchanged. In contrast, the peak intensity of quartz seems to increase after treatment at 90 °C. This finding suggests that the part of amorphous phase have dissolved to contribute an increased quartz concentration.

Further treatment of the raw fly ash at 140 °C yielded the hydrated compounds close to the synthetic minerals of tobermorite-11 Å ($Ca_5Si_6O_{18}{\cdot}5H_2O$) and illite [$KAl_3Si_3O_{10}(OH)_2$], as can be estimated from the peaks at 7.82° 2θ (PDF#45-1480) and 10.27° 2θ (PDF#26-091), respectively. Taking the positions of other peaks into account, Al-substituted tobermorite-11 Å seems to be the most likely candidate with structural formula [$Ca_5Na_xAl_xSi_{6-x}(OH)_2O_{16}{\cdot}4H_2O$] [23,30]. In addition, a hydrogarnet mineral close to katoite [$Ca_3Al_2(SiO_4)(OH)_8$] could be observed in the XRD trace at 32.31° 2θ (PDF# 84-0917). The formation of katoite may be related to the excess of Al-ion as can be estimated from the molar component ratios of CaO/[$SiO_2 + Al_2O_3$] and Al/[Al + Si], respectively. The ratios calculated from the XRF data of the raw sample provided values of 1.53 and 0.37 respectively, which are beyond the values required for the optimum yields of Al-substituted tobermorite-11 Å [24]. Furthermore, analcime (PDF#89-6324), hydroxylcancrinite (PDF#88-1931) and Sodalite (PDF#88-2088) developed up to the temperature of 140 °C, in addition to gypsum ($CaSO_4{\cdot}2H_2O$) (PDF#76-1746). In this stage, proportions of hydrocalumite and monosulfate decreased with increasing temperature, whereas the gypsum and tobermorite-11 Å contents increase.

The formation of Al-substituted tobermorite-11 Å was also confirmed by SEM/EDX analysis. A platy or lath-like morphology developed in the raw sample treated at 180 °C is a typical synthetic tobermorite-11 Å crystallite (Fig. 2a) [23,24]. Additionally, the resulting tobermorite-11 Å structure may accommodate cation of Zn^{2+} as shown by the EDX spectrum (Fig. 2b).

For KOH activation, the raw sample similarly treated with 0.5 M at temperature ranges tested (90–180 °C) for 48 h is shown in Fig. 1b. At 90 °C, peaks of halite, anhydrite and sylvite were clearly absent; correspondingly new peaks of hydrocalumite and monosulfate appeared. Up to a temperature of 140 °C, a mixed product of Al-substituted tobermorite-11 Å and katoite was observed. With increasing temperature, mineralogical phase compositions of the raw sample were altered as a result of the dissolution of some minerals (*e.g.*, NaCl and KCl) and the formation of new secondary precipitates (*i.e.*, hydrocalumite and monosulfate). Treated

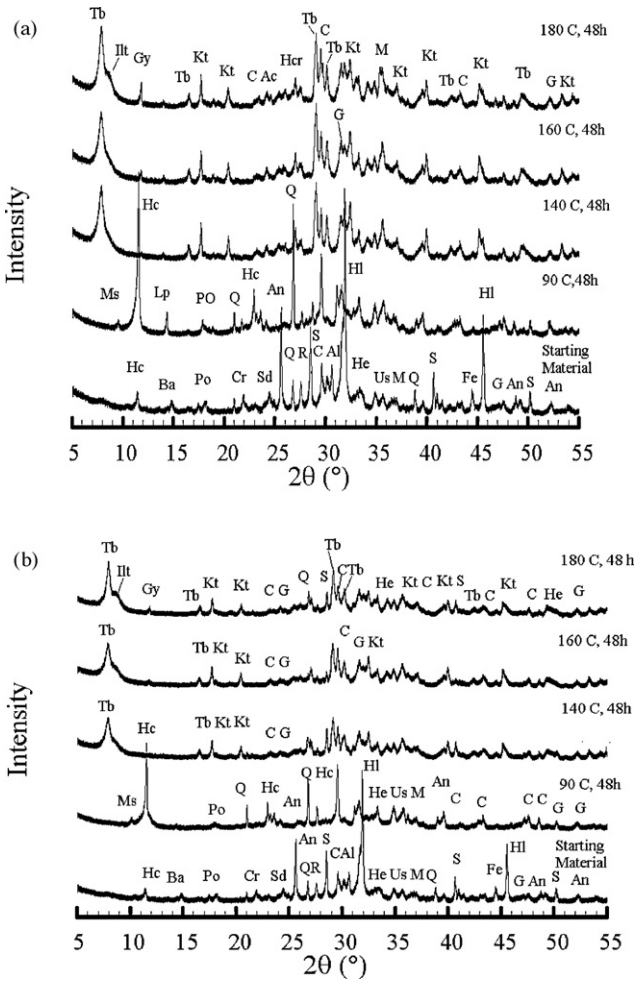

Fig. 1. XRD patterns of fly ash treated at various temperatures for 48 h in (a) 0.5 M NaOH, and (b) 0.5 M KOH. The peaks are labelled Ac (analcime), Al (alunite), An (anhydrite), Ba (bassanite), C (calcite), Cr (cristobalite), Fe (iron), G (gehlenite), Gy (gypsum), Hc (hydrocalumite), Hcr (Hydroxylcancrinite), He (hematite), Hl (halite), Ilt (illite), Kt (katoite), Lp (lepidocrocite) M (magnetite), Ms (monosulfate), Po (portlandite), Q (quartz), R (rutile), S (sylvite), Sd (sodalite), Us (ulvöspinel) and Tb (tobermorite-11 Å).

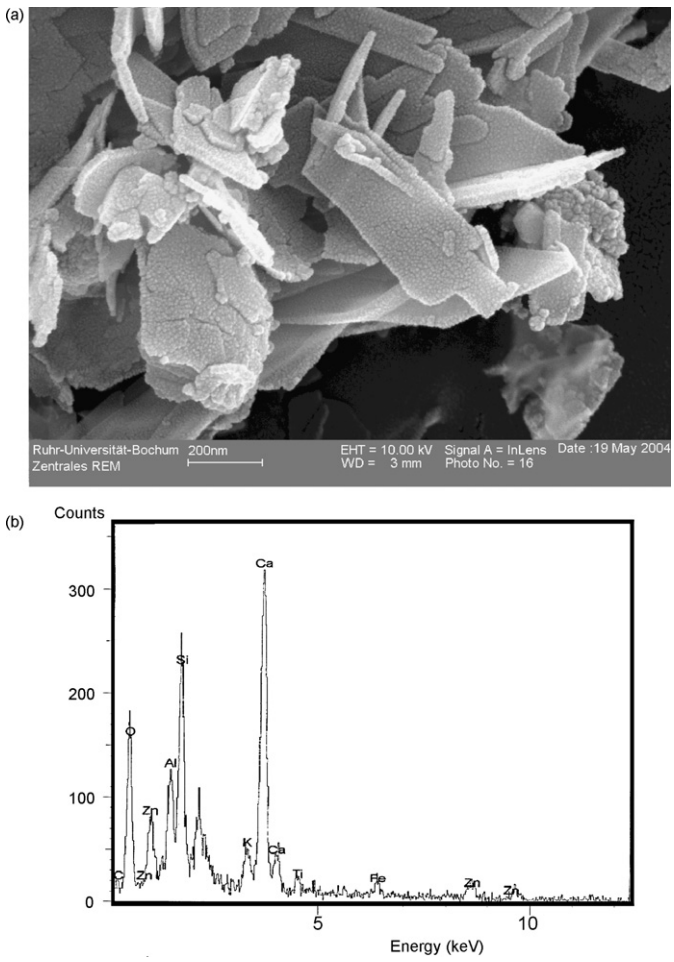

Fig. 2. (a) SEM image of a platy network Al-substituted tobermorite-11 Å crystal morphology, and (b) EDX spectrum obtained from fly ash hydrothermally treated in 0.5 M NaOH at 180 °C for 48 h.

at 160 °C, gypsum was formed, accompanied by the depletion of hydrocalumite and monosulfate.

Reactivity of aluminosilicates during the hydrothermal process was evaluated by the XRD Rietveld method as a function of temperature (Fig. 3a). At a temperature of 90 °C, there is evidence for the reduction of the glass content and an increased amount of quartz, compared to those in the starting material. However the quartz content then reduced gradually with rising temperature. The major phases arising from the treatment at 140 °C were found to be tobermorite-11 Å and katoite, but only minor amounts of zeolites, *i.e.* analcime and hydroxylcancrinite, were produced. Starting at a temperature of 160 °C, minor amounts of illite and gypsum developed. Moreover, the hydrothermal treatment at 180 °C yielded a relatively high abundance of tobermorite-11 Å (21.8 wt.%), illite (8.9 wt.%) and katoite (4.7 wt.%).

The reactivity of aluminosilicates in 0.5 M KOH for 48 h at temperature ranges between 90 and 180 °C was also observed (Fig. 3b). The amount of glassy phase reduces while the quartz content increases at 90 °C. Hydrothermal treatment at 140 °C produced significant amounts of tobermorite-11 Å (11.0 wt.%), illite (8.2 wt.%) and katoite (4.9 wt.%). Up to 160 °C, tobermorite-11 Å and katoite became the major products. By treating at 180 °C, only minor amounts of zeolitic materials (*i.e.*, analcime and hydroxylcancrinite) could be generated, suggesting that the synthesis process was relatively insensitive to the raw fly ash compositions, more so a function of temperature and time [18,23]. From the quantitative XRD results (Fig. 3a and b), the extent of reaction for fly ash in the presence of KOH was considerably lower than that in the presence of NaOH, especially for the formation of tobermorite-11 Å and katoite. Upon treatment at 180 °C, no remarkable reduction of the glassy content was noted, while the tobermorite-11 Å content remained constant. Insignificant changes in the amounts of analcime, hydroxylcancrinite, and illite with rising reaction temperature were also observed.

Based on the results of the hydrothermal treatments of fly ash in the respective range of 90–180 °C in 0.5 M NaOH for 48 h, the following scenario may be envisaged:

(i) The amorphous content is dissolved during hydrothermal treatment at 90 °C and the major phase of hydrocalumite is formed while the quartz content increases.
(ii) At an intermediate temperature (140–160 °C), tobermorite-11 Å and katoite as well as a few of zeolitic materials are initially formed.
(iii) At high temperature (180 °C), Ca, Al and Si ions, which are available in the amorphous phase, contribute to the formation of clay "illite", katoite and tobermorite-11 Å.

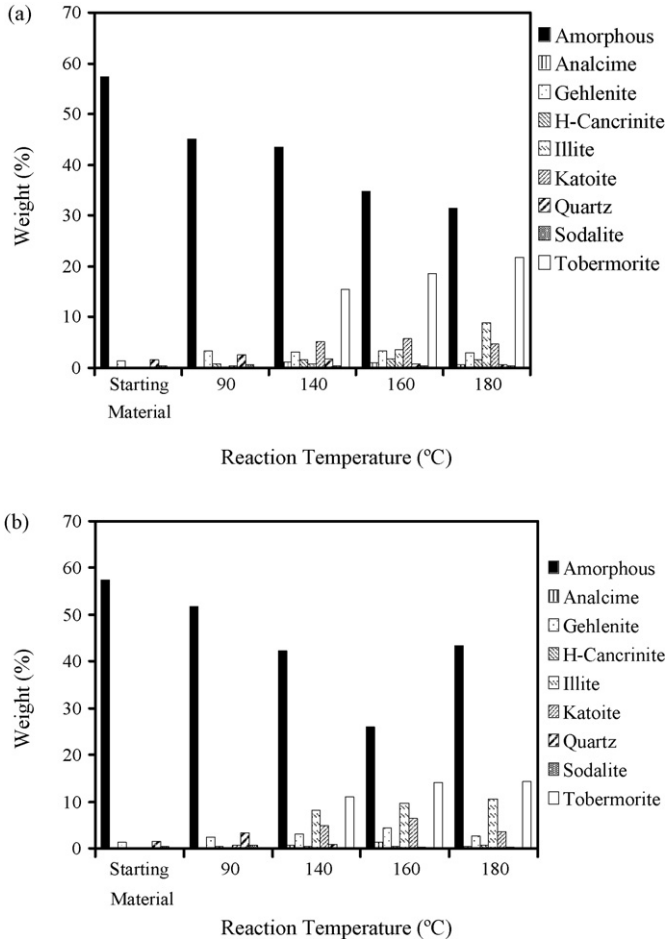

Fig. 3. Reactivity of aluminosilicates during the hydrothermal processing of fly ash in (a) 0.5 M NaOH, and (b) 0.5 M KOH at different reaction temperatures and fixed time of 48 h. *Note*: H-Cancrinite: hydroxylcancrinite.

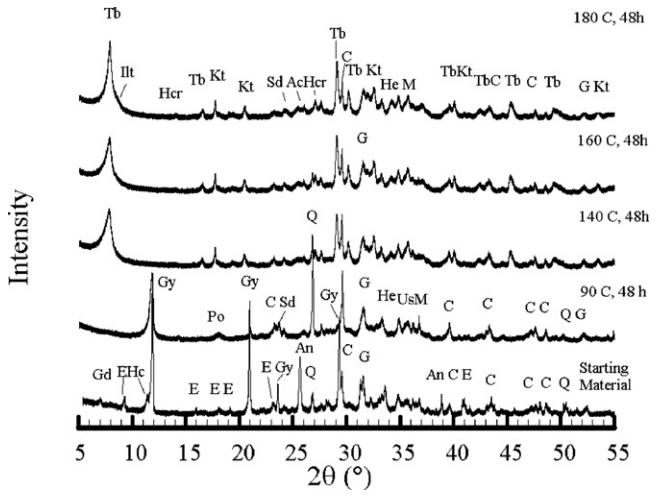

Fig. 4. XRD patterns of the washed fly ash treated at various temperatures in 0.5 M NaOH for 48 h. The peaks are labelled Ac (analcime), An (anhydrite), C (calcite), E (ettringite), G (gehlenite), Gd (gordaite), Gy (gypsum), Hc (hydrocalumite), Hcr (hydroxylcancrinite), He (hematite), Ilt (illite), Kt (katoite), M (magnetite), Po (portlandite), Q (quartz), Sd (sodalite), Tb (tobermorite-11 Å) and Us (ulvöspinel).

3.2. Hydrothermal processing of washed fly ash

The washed fly ash is composed of a significant amount of amorphous phase and various SiO_2 and Al_2O_3 bearing phases such as quartz and gehlenite (Table 2). More than 40 wt.% of washed fly ash consisted of probably a silica-rich glasslike phase. A number of hydrated phases such as ettringite and gypsum, which developed after washing fly ash, are regarded as impurities for the present study as they do not contribute to formation of zeolites or neomorphic phases. Moreover, the synthesis of tobermorite-11 Å and other zeolitic materials using the washed fly ash under various temperatures and a fixed condition (0.5 M NaOH for 48 h) was examined by XRD (Fig. 4). At 90 °C, the disappearance of gordaite, ettringite and hydrocalumite is evident, while gypsum is still present. Additionally, the reflection of quartz shows an increase in intensity. However, a number of the remaining parent phases such as gehlenite, calcite and portlandite remained stable and therefore they did not react in the alkali solution.

Further formation of tobermorite-11 Å and katoite was initially observed after treatment at 140 °C. Moreover, the peak intensity of quartz was greatly lowered. This finding indicated that the silicate from quartz may have dissolved in the NaOH solution to form hydrogels, which is responsible for the formation of tobermorite-11 Å, katoite and a few of zeolites such as analcime and hydroxylcancrinite. On the other hand, gehlenite remained unchanged after the reactions. The washed fly ash treated at 180 °C resulted in the highest production of tobermorite-11 Å, as indicated by the highest intensity peak at 7.81° 2θ (PDF#45-1480) together with the formation of illite.

The formation of Al-substituted tobermorite-11 Å in the hydrothermal product of the washed fly ash acquired at 180 °C for 48 h has been confirmed by SEM analysis, showing the existence of the typical platy morphology that is commonly found for synthetic tobermorite (Fig. 5a). The evidence of 11 Å mineral, which is very likely tobermorite, is also confirmed by X-ray diffractogram presented previously in Fig. 1a.

The mixed product of Al-substituted tobermorite-11 Å and katoite formed in the treated washed fly ash could be controlled by a typical range of the Ca/(Si + Al) and the Al/(Al + Si) ratios. These ratios were computed from the XRF data to be 1.77 and 0.27, respectively. These values are beyond of the ranges of (0–0.17) and (0.80–0.85), respectively, which are considered optimal for the synthesis of tobermorite-11 Å [24,30]. Evidently, katoite is the co-product of tobermorite-11 Å which might also contain Zn^{2+} as revealed by EDX (Fig. 5b).

3.3. Stability of minerals in the raw fly ash and treated fly ash under acidic conditions

XRD was used to provide a first (*qualitative*) explanation for the toxicity of materials related to the metal leaching-controlling phases. Table 3 provides the lead-bearing minerals which were identified in the raw fly ash: minium (Pb_3O_4) and caracolite [$Na_3Pb_2(SO4)_3Cl$], while Zn is present in $ZnCl_2$. The XRD pattern of the leached raw fly ash from the TCLP test is shown in Fig. 6a. No peaks of caracolite are evident in the leached fly ash. Similarly, $ZnCl_2$ disappeared, so that these phases were dissolved in the leaching solution. Apparently, the crystalline phases, which accommodate some amounts of Pb and Zn, have a lower leaching resistance, thereby leading to the high potential toxicity of the material.

Further, chloride minerals (NaCl, and KCl) detected in the raw fly ash disappeared. Consequently, an increase of the relative content of insoluble minerals in the leached sample is noted. Clearly, anhydrite is a less soluble phase [31] and its diffraction peak intensities increase as evidenced by an additional peak at 25.45° 2θ (PDF#86-2270). A rapid formation of gypsum ($CaSO_4{\cdot}2H_2O$) in the leached sample was also observed, likely due to the dissolution of hydrocalumite and bassanite.

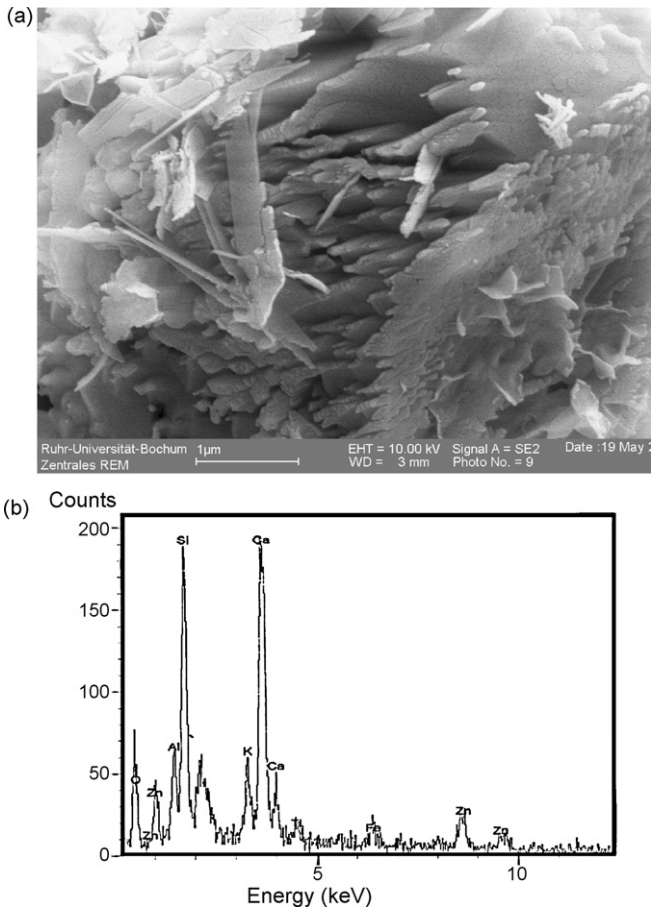

Fig. 5. (a) SEM image of a platy network Al-substituted tobermorite-11 Å crystal morphology, and (b) EDX spectrum for the hydrothermal product of the washed fly ash in 0.5 M NaOH at 180 °C for 48 h.

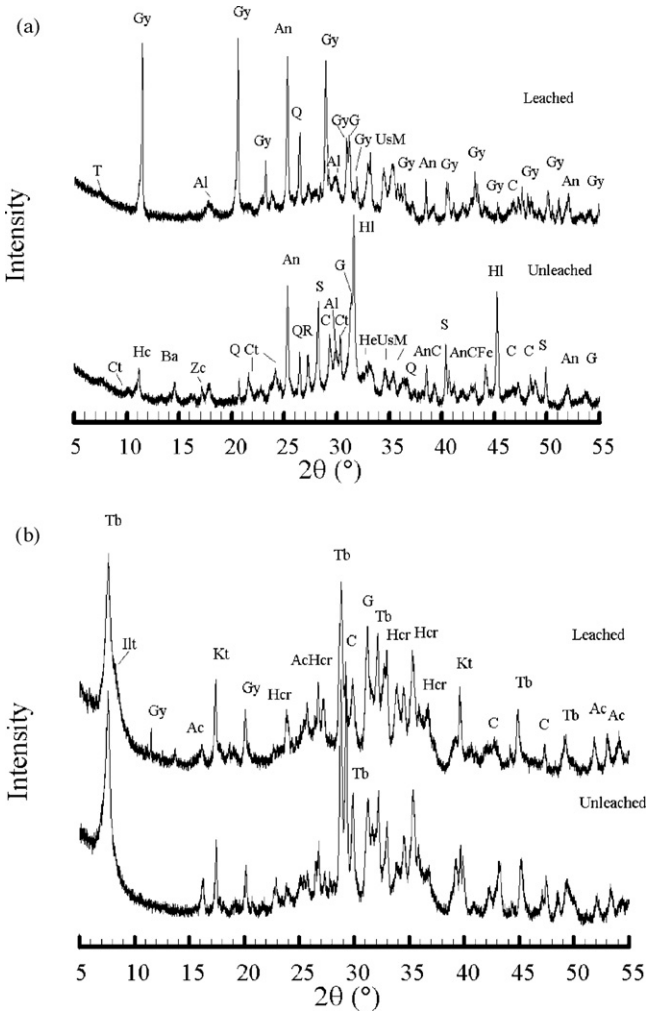

Fig. 6. XRD patterns of (a) unleached and leached fly ash and (b) unleached and leached hydrothermal product of fly ash. The peaks are labelled Ac (analcime), Al (alunite), An (anhydrite), Ba (bassanite), C (calcite), Cr (cristobalite), Ct (caracolite), Fe (iron), G (gehlenite), Go (goethite), Gy (gypsum), Hc (hydrocalumite), Hcr (hydroxylcancrinite), He (hematite), Hl (halite), Ilt (illite), Kt (katoite), M (magnetite), Ms (monosulfate), Q (quartz), R (rutile), S (sylvite), T (tobermorite-14 Å), Tb (tobermorite-11 Å), Us (ulvöspinel) and Zc ($ZnCl_2$).

Fig. 6b shows the leached hydrothermal products presenting strong XRD peaks with some modifications of the patterns with respect to the unleached minerals. Sulfates, aluminosilicates, carbonates and oxides are still present, but sylvite and halite are absent. It appears that the release of K^+, Na^+ and Cl^- may be solely controlled by the solubility of halite and sylvite. The XRD analysis of the leached samples proved that tobermorite-11 Å, and katoite together with illite, analcime and hydroxylcancrinite have a high leaching resistance in the acidic solution. It also provides evidence that no significant alteration of the main mineral compositions is observed, except for the absence of chloride minerals (*e.g.*, halite and sylvite). Consequently, the present results show that the hydrothermal treatment of fly ash would generate a low leachability of the minerals.

Table 3 summarises the TCLP results, along with the limit concentrations of the heavy metals established by the US law for solid waste disposal. For the raw fly ash, Cd, Pb and Zn concentrations in the leaching solution exceeded the TCLP limits. It appears reasonable that the high leaching characteristics of Zn and Pb are due to the likely fact that most Zn and Pb are incorporated in the highly soluble minerals (*e.g.*, $ZnCl_2$ and caracolite), which have a lower chemical resistance than the amorphous phases [6]. Additionally, the high leaching of Cd may be influenced by solubility-controlling minerals such as $Cd_5(AsO_4)_3Cl$ and $CdCO_3$ as proposed by Eighmy et al. [32], although specific Cd-bearing minerals were not detected by XRD, likely they are present below the detection limit. However, concentrations of Cu, Cr, Ni and As in the leaching solution from most raw fly ash samples have passed the TCLP tests.

Table 3
Heavy metal concentrations in the leaching solution after TCLP test.

Sample	Cu	Cd	Cr	Ni	Pb	Zn	As	pH
	ppm							
Raw fly ash	14	12	1	3	17	397	0.212	5
Hydrothermal product of raw fly ash	1	1	1	1	1	27	0.019	7
Washed fly ash	138	35	3	9	393	1504	0	5
Hydrothermal product of washed fly ash	2	5	2	3	2	0	0	6
TCLP limit	100	1	5	100	5	5	5	

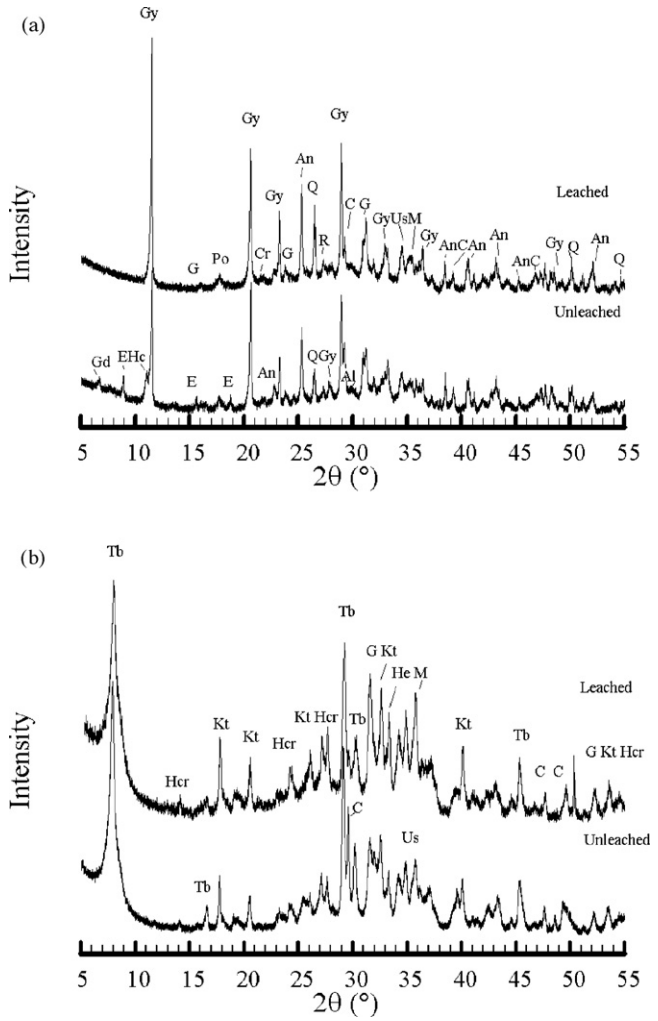

Fig. 7. XRD patterns of (a) unleached and leached-washed fly ash and (b) unleached and leached hydrothermal product of washed fly ash. The peaks are labelled Ac (analcime), Al (alunite), An (anhydrite), C (calcite), Cr (cristobalite), E (ettringite), G (gehlenite), Gd (gordaite), Gy (gypsum), Hc (hydrocalumite), Hcr (hydroxylcancrinite), He (hematite), Ilt (illite), Kt (katoite), M (magnetite), Po (portlandite), Q (quartz), R (rutile), Tb (tobermorite-11 Å) and Us (ulvöspinel).

3.4. Stability of minerals in the washed fly ash and treated washed fly ash under acidic conditions

A large weight fraction of hydrate phases found in the washed fly ash are hydrocalumite, ettringite and gordaite $[NaZn_4(SO_4)(OH)_6Cl(H_2O)_6]$ (Table 2). However, these hydrate phases, except for gypsum, disappear after leaching (Fig. 7a). This agrees with previous studies showing that hydrocalumite and ettringite are unstable in the solution with the pH ranges of 5–7 [30,33]. Further, there is a relative increase of peak intensities of some minerals such as anhydrite, quartz and gehlenite, relative to those in the unleached sample.

Further, XRD analyses conducted before leaching indicated that hydrothermal products of the washed fly ash contained tobermorite-11 Å and katoite as the dominant phases plus minor zeolitic materials. After leaching, the diffractograms indicated that no alteration of major phases occurred in the leached specimens (Fig. 7b). As expected, the hydrothermal products of the washed fly ash contained stable minerals including quartz, anhydrite, gehlenite and gypsum. This evidence agrees very well with the previous findings for the leached hydrothermal products of the raw fly ash.

Table 3 presents the TCLP results for the heavy metal concentrations in the leaching solution from the washed fly ash and the treated material. It is noted here that As was not detected in the leaching solution. For the investigation of washed fly ash, the concentrations of some heavy metals (Zn, Pb, Cu and Cd) in the solution exceed the TCLP limits. The high heavy metal leaching from the washed fly ash may be also influenced by the high initial contents of the heavy metals in the starting material (Table 1). This is because the washed fly ash is generally enriched in heavy metals after washing [34]. Furthermore, the leaching behaviour of the washed fly ash could be explained by recalling that the mobilization of the particular heavy metal (Zn, Pb and Cd) is influenced by the stability of hydrate phases (*i.e.,* ettringite and hydrocalumite). Ettringite and hydrocalumite are probably soluble phases controlling leaching, in particular of Cd^{2+}, Pb^{2+}, and Zn^{2+}-ions at the pH values examined. In contrast, the concentrations of Cr and Ni in the leachate are below the limits, suggesting that these elements may be distributed in the amorphous phase, alloys (Fe-Cr-Ni) or spinel. Additionally, the leaching evaluation of the hydrothermal product of the washed fly ash indicates that concentrations of Zn, Pb and Cd in the solution were below the TCLP limits. It suggests that a significant part of Zn and Pb could be incorporated into tobermorite-11 Å, katoite, zeolites and possibly amorphous silicate phases as evidenced by SEM/EDX analysis.

4. Discussion

The results presented here prove that the studied MSWI fly ash contains significant proportions of crystalline and glass phases that could be determined by XRD Rietveld analysis (Table 2). The major glassy materials are particularly present in the fly ash as a consequence of melt droplets formed through condensation of the flue gases [4,32]. In addition to glass phase, magnetite and melilite, as well as some silicates are identified. Also the formation of chloride minerals such as NaCl, and KCl, which have been previously reported by Eighmy et al. [32] is evident. Several processes occurred during incineration such as vaporisation, melting, crystallisation, vitrification, condensation, precipitation, and the flue gas clean up are supposed to influence the formation of complex mineralogy in the fly ash [4,32]. Some heavy metals appear to be preferentially associated with a specific mineralogy. Lead and zinc are volatile at the incinerator temperature (850–1000 °C) and could be identified in the crystalline form of minium (Pb_3O_4), caracolite $[Na_3Pb_2(SO_4)_3Cl]$, and zinc chloride ($ZnCl_2$).

A simple synthetic route to the formation of tobermorite-11 Å, katoite and minor amounts of zeolites by hydrothermal treatments of MSWI fly ash has been demonstrated. The main results of Al-substituted tobermorite-11 Å and katoite have been shown to be consistent and in agreement with previous experimental research of using waste materials [18,22–24]. In addition, small quantities of illite, analcime and hydroxylcancrinite were produced from the raw fly ash by changing the synthesis parameters such as temperature and the activation solution.

Mineralizing agents can be used to control the relative abundance of potentially competing hydrothermal reaction products. In our study, NaOH was found to promote the rapid decomposition of the parent material of fly ash and subsequent formation of the mixed minerals of Al-substituted tobermorite-11 Å and katoite. An equivalent concentration of KOH resulted in a comparatively slower rate of decomposition of the parent phases and promoted the formation of Al-substituted tobermorite-11 Å with smaller proportions of katoite.

An examination of the current literature indicates that there are three phases in MSWI fly ash being a very important for contributing the aluminium and silicon to hydrothermal syntheses: (i) amorphous aluminosilicate glass, (ii) quartz (iii) gehlenite

[18,23,24]. Our study revealed that the aluminosilicate glass phase is the most abundant and most unstable phase in the hydrothermal environment. Accordingly it has the highest rate of dissolution and it is the largest contributor of aluminium and silicon to the hydrothermal products. There is also a general reduction in the quartz content during hydrothermal treatments. However, gehlenite did not react with alkali solution to form zeolites and other neomorphic phases. The residual non-reacted components of fly ash corresponding to Ca-sulfate bearing minerals, carbonate, magnetite, ulvöspinel and hematite remained unchanged during the hydrothermal treatments.

The synthesis strategy employing the washed fly ash yielded a similar mixed product of tobermorite-11 Å and katoite with minor amounts of analcime and hydroxylcancrinite. The ratio of Si/Al has been considered to be the most important factor for the development of zeolitic materials, while synthesis parameters (*i.e.,* time and reaction temperature) played a smaller role. According to Coleman and Brassington [24] the optimum yield of Al-substituted tobermorite-11 Å could be generally achieved from the reaction compositions falling within the following molar component ratios:

$$0.80 < \frac{\mathrm{CaO}}{|\mathrm{SiO_2} + \mathrm{Al_2O_3}|} < 0.85 \quad (1)$$

$$0.00 < \frac{\mathrm{Al}}{\mathrm{Al} + \mathrm{Si}} < 0.17 \quad (2)$$

It has been reported by Coleman and Brassington [24] that reaction times and proportions of aluminium and calcium have a significant influence on the production of Al-substituted tobermorite-11 Å. However, the long reaction times and an increased proportion of aluminium and calcium would promote the formation of hydrogarnet katoite and other calcium silicate hydrate (CSH) as additional phases to Al-substituted tobermorite-11 Å. Hence, the flexibility of hydrothermal processing affords a possibility for controlling composition and morphology of the product phases. Accordingly, the yield and extent of Al-substituted tobermorite-11 Å product phase derived from MSWI fly ash could be modified by an appropriate manipulation of reagent compositions and reaction conditions in order to maximize its ion exchange performance.

Further, the molar component ratios of our fly ash (Eqs. (1) and (2)) as calculated from the XRF data (Table 1) are beyond the above values. Accordingly, an improved yield of tobermorite could be expected from the stoichiometric additions of a reactive source of silica and a calcium oxide to adjust the composition to within the optimal ranges quoted above. However, the development of tobermorite-11 Å from MSWI fly ash for marketable sorbents requires a degree of *compromise* between the effectiveness of the product in a given application and the cost and the complexity of processing. The use of an additional feedstock material and processing steps generally implies an additional cost, which requires compensating by the improved service performance.

The leaching analysis of the MSWI fly ash indicates that the materials are hazardous. The XRD technique has been employed for the identification of solubility-controlling phases. It is well established that the matrix compositions of fly ash could substantially control the leaching of metals. This can be observed in part for the higher leachability of Cd which is probably related to the dissolution of NaCl and KCl [35]. Additionally, $ZnCl_2$ and hydrocalumite might be responsible for the leaching of zinc, while a part of lead leaching was possibly promoted by the dissolution of caracolite. The dissolution of hydrocalumite from the raw fly ash resulted in the precipitation of a large amount of gypsum. However, the hydrothermal products behaved quite differently in that they were quite resistant in the acidic solution. Tobermorite-11 Å, katoite and zeolitic compounds are still present in the leached sample of the hydrothermal product. As the raw fly ash was enriched with chlorides, the residual mineral contents in the hydrothermal product are increased by the dissolution of halite and/or sylvite after leaching.

Further, the leaching characteristic of the washed fly ash is mainly influenced by the presence of gordaite, gypsum, hydrocalumite and ettringite. The XRD analysis of the leached washed fly ash provided evidence of the dissolution of gordaite, hydrocalumite and ettringite in the acidic solution. But gypsum remained stable in the materials. Importantly, there is no significant difference between the leaching characteristics of the hydrothermal product from the washed fly ash and the raw fly ash. The results also demonstrated that hydrothermal products of the washed fly ash displayed superior mineral stability in the acidic environment.

Further, pH is the main experimental condition influencing the heavy metal release; the lower the pH, the greater the heavy metal release. Zn and Pb are amphoteric with hydroxyl complexation, exhibiting increased solubility under strongly acidic conditions [2]. Our study confirms the findings of the experiments that the acidity of the leaching solution had an impact on the solubility of metals, especially zinc and lead. The results also show that a significant amount of cadmium was dissolved in the acidic leaching solution and this agrees very well with the expected behaviour reported in the literature [36]. Therefore the acidic solution can be used for a partial extraction and recovery of lead and zinc from the fly ash, but not for ultimate detoxification of the fly ash. It is suggested that leaching tests over wide ranges of pH values with the use of extraction fluid will be completed to fully understand the complexity of leaching resistance in these materials.

Use of an acidic leaching solution for fly ash clearly reduced the TCLP concentration of Pb [36], but a thermal treatment of the fly ash at extremely high temperatures (>850 °C) is required to break down dioxins completely. The dioxin levels of our materials comply with the limit value of 0.1 ng TEQ/m^3 (the toxic equivalent concentration), according to the Ordinance on Waste Incineration Plants, and they do not exceed the legal limits for deposition of the fly ash on a dedicated disposal site in Germany. Treatment of the fly ash at the extremely high temperature necessary to destroy the dioxins completely would mobilize some other toxic volatiles which would need to be recaptured. This would naturally have implications for an economic analysis of the treatment, which, however, has been outside the scope of this work.

Hydrothermal treatments of the raw and the washed fly ash samples had an evident impact on the reduced leaching of metals, in that all metals showed a marked reduction in the leaching concentrations. It is supposed that the observed reduction in mobilization of heavy metals is caused by the incorporation of metals in phases with low solubility. For example, Zn, Pb and Cd may be incorporated in tobermorite-11 Å, katoite and amorphous alumosilicate phase. Accordingly, the hydrothermal method is very promising for the development of chemically stabilized products. Nevertheless, from the economic of point of view, the cost for hydrothermal treatments should be relatively lower than that for high temperature volatilization and evaporation of heavy metals or vitrification.

Furthermore, this paper has not attempted to deal with transfer of dioxin in the fly ash during the hydrothermal processing. Principally fly ash from incinerators tends to contain unburnt carbon, persistent organic pollutants (POP), and heavy metals. The POP typically represents polychlorinated dibenzo-p-dioxins and furans (PCDD/F), chlorobenzenes and chloronaphthalenes. In Germany, these organic pollutants are destroyed by a thermo-catalytic process with significant reduction of the toxic equivalent concentration (TEQ) by more than 99% [37]. In the present case, the dioxin concentration in fly ash is considered sufficiently low to influence the mineral phases. However, work remains to be carried out to investigate the behaviour of POPs during hydrothermal processing.

The observed formation of zeolithic minerals of high surface area provides some adsorptive potential for POPs.

5. Conclusion

It can be concluded that the hydrothermal treatment of fly ash in the alkali solutions of 0.5 M NaOH at 180 °C for 48 h produced significant amounts of tobermorite-11 Å and katoite in addition to small quantities of hydroxylcancrinite and analcime. The heavy metals may be either absorbed or physically encapsulated in the stable mineral phases. The water washing treatment of fly ash provides no significant difference in yielding tobermorite-11 Å and katoite. The transformation of fly ash into tobermorite-11 Å, katoite, and zeolitic compounds is significant as it opens new opportunities for this type of waste, which can be used among other for immobilizing other toxic and radioactive wastes in cement and asphalts. This indicates that the hydrothermal method provides a promising solution to the reduction of environmental hazards of fly ash deposits and it opens opportunities for giving value to the fly ash as a resource.

Acknowledgements

The authors wish to thank Dr. Neuser for their help in collecting electron microscope analysis data. Special thank to Dr. Reinecke for his support in the XRD laboratory. The assistance of Hendrik Narjes, Astrid Michele and Sandra Grabowski performing laboratory experiments is also gratefully acknowledged.

References

[1] O. Hjelmar, Disposal strategies for municipal solid waste incineration residues, J. Hazard. Mater. 47 (1996) 345–368.
[2] T. Sabbas, A. Polettini, R. Pomi, T. Astrup, O. Hjelmar, P. Mostbauer, G. Cappai, G. Magel, S. Salhofer, C. Speiser, S. Heuss-Assbicher, R. Klein, P. Lehner, Management of municipal solid waste incineration residues, Waste Manage. 23 (2003) 61–88.
[3] K. Akiko, N. Yukio, I. Teruji, Chemical speciation and leaching properties of elements in municipal incineration ashes, Waste Manage. 16 (1996) 523–536.
[4] L.L. Forestier, G. Libourel, Characterization of flue gas residues from municipal solid waste combustors, Environ. Sci. Technol. 32 (1998) 2250–2256.
[5] C. Ferreira, A. Ribeiro, L. Ottosen, Possible applications for municipal solid waste fly ash, J. Hazard. Mater. B96 (2003) 201–216.
[6] J.M.A. Rincon, M. Romero, A.R. Boccaccini, Microstructural characterisation of a glass and a glass-ceramic obtained from municipal incinerator fly ash, J. Mater. Sci. 34 (1999) 4413–4423.
[7] M. Erol, S. Kücükbayrak, A. Ersoy-Mericboyu, M.L. Övecoglu, Crystallization behaviour of glasses produced from fly ash, J. Eur. Ceram. Soc. 21 (2001) 2835–2841.
[8] Y.J. Park, J. Heo, Nucleation and crystallization kinetics of glass derived from incinerator fly ash waste, Ceram. Int. 28 (2002) 669–673.
[9] Y.J. Park, J. Heo, Vitrification of fly Ash from municipal solid waste incinerator, J. Hazard. Mater. B91 (2002) 83–93.
[10] M.A. SØrensen, B.C. Koch, M.M. Stackpoole, R.K. Bordia, M.M. Benjamin, T.H. Christensen, Effects of thermal treatment on mineralogy and heavy metal behaviour in iron oxide stabilized air pollution control residues, Environ. Sci. Technol. 34 (2000) 4620–4627.
[11] K.J. Hong, S. Tokunaga, Y. Ishigami, T. Kajiuchi, Extraction of heavy metals from MSW incinerator fly ash using saponins, Chemosphere 41 (2000) 345–352.
[12] K.J. Hong, S. Tokunaga, T. Kajiuchi, Extraction of heavy metals from MSW incinerator fly ashes by chelating agents, J. Hazard. Mater. B75 (2000) 57–73.
[13] H. Katsuura, T. Inoue, M. Hiraoka, S. Sakai, Full-scale plant study on fly ash treatment by the acid extraction process, Waste Manage. 16 (1996) 491–499.
[14] F.P. Glasser, Fundamental aspects of cement solidification and stabilization, J. Hazard. Mater. 52 (1997) 151–170.
[15] A. Nzihou, P. Sharrock, Calcium phosphate stabilization of fly ash with chloride extraction, Waste Manage. 22 (2002) 235–239.
[16] P. Ubbriaco, D. Calabrese, Hydration behaviour of mixtures of cement and fly ash with high sulphate and chloride content, J. Therm. Anal. Cal. 61 (2000) 615–623.
[17] P. Ubbriaco, P. Bruno, A. Traini, D. Calabrese, Fly ash reactivity: formation of hydrate phases, J. Therm. Anal. Cal. 66 (2001) 293–305.
[18] X. Querol, N. Moreno, J.C. Umaña, A. Alastuey, E. Hernández, A. López-Soler, F. Plana, Synthesis of zeolites from coal fly ash: an overview, Inter. J. Coal Geology 50 (2002) 413–423.
[19] J.D. Rimstidt, H.L. Barnes, The kinetics of silica-water reactions, Geochim, Cosmochim. Acta 44 (1980) 1683–1699.
[20] G.C.C. Yang, T.Y. Yang, Synthesis of zeolites from municipal incinerator fly Ash, J. Hazard. Mater. 62 (1998) 75–89.
[21] H. Maenami, H. Shin, H. Ishida, T. Mitsuda, Hydrothermal solidification of wastes with formation of zeolites, J. Mater. Civil Eng. 12 (2000) 302–306.
[22] M. Miyake, C. Tamura, M. Matsuda, Resource recovery of waste incinerator fly ash: synthesis of zeolites A and P, J. Am. Ceram. Soc. 85 (2002) 1873–1875.
[23] Z. Yao, C. Tamura, M. Matsuda, M. Miyake, Resource recovery waste incineration fly ash: synthesis of tobermorite as ion exchanger, J. Mater. Res. 14 (1999) 4437–4442.
[24] N.J. Coleman, D.S. Brassington, Synthesis of Al-substituted 11 Å tobermorite from newsprint recycling residue: a feasibility study, Mater. Res. Bull. 38 (2003) 485–497.
[25] A.P. Bayuseno, Mineral phases in raw and processed municipal waste incineration residues—towards a chemical stabilisation and fixation of heavy metals, Ph.D. Thesis. Ruhr-Universität Bochum, Germany, 2006.
[26] H.M. Rietveld, A profile refinement method for nuclear and magnetic structures, J. Appl. Cryst. 2 (1969) 65–71.
[27] SIROQUANT, Quantitative XRD phase analysis software based on the Rietveld method, CSIRO, Australia, Version 2.5, 2002.
[28] R.J. Hill, C.J. Howard, Quantitative phase analysis from neutron powder diffraction data using the Rietveld method, J. Appl. Cryst. 20 (1987) 467–474.
[29] U.S. EPA, Part 261, Appendix II—Method 1311 Toxicity characteristic leaching procedure (TCLP), Federal Register, vol. 55, no. 61, March 29, 1990, Rules and Regulations, 1990, pp. 11863–11877.
[30] H.F.W. Taylor, Cement Chemistry, Academic Press, London/New York, 1990.
[31] K.S. Wang, K.Y. Chiang, K.L. Lin, C.J. Sun, Effects of a water-extraction process on heavy metal behaviour in municipal solid waste incinerator fly ash, Hydrometallurgy 62 (2001) 73–81.
[32] T.T. Eighmy, J.D. Eusden, J.E. Krzanowski, D.S. Dominggo, D. Stampfli, J.R. Martin, P.M. Erickson, Comprehensive approach toward understanding element speciation and leaching behaviour in municipal solid waste incineration electrostatic precipitator ash, Environ. Sci. Technol. 29 (1995) 629–646.
[33] S. Rémond, D.P. Bentz, P. Pimienta, Effects of the incorporation of municipal solid waste incineration fly ash in cement pastes and mortars II: modeling, Cement Concrete Res. 32 (2002) 565–576.
[34] T. Mangialardi, Disposal of MSWI fly ash through a combined washing-immobilisation process, J. Hazard. Mater. B98 (2003) 225–240.
[35] C. Brunori, S. Balzamo, Morabito, Comparison between different leaching tests for the evaluation of metal release from fly ash, Fresenius J. Anal. Chem. 371 (2001) 843–848.
[36] Z. Youcai, L. Song, L. Guojian, Chemical stabilization of MSW incinerator fly ashes, J. Hazard. Mater. B95 (2002) 47–63.
[37] R. Stuetzle, H. Hagenmaier, O. Hasenkopf, G. Schettle, Erste Erfahrungen mit der Demonstrationsanlage in der MVA Stuttgart-Muenster zum Abbau von PCDD und PCDF in Flugaschen, VGB Kraftwerkstechnik 71 (1991) 1038–1040.